# Diagnosis of Multiple Bearing Faults in BLDC Motors Using ReliefF Feature Selection and Random Forest Classifier

Meiyanto Eko Sulistyo [1,2], Didik Djoko Susilo [1,*], Muhammad Nizam [2], Ubaidillah [1], and Felly Anta [1]

[1] Department of Mechanical Engineering, Universitas Sebelas Maret, Surakarta, Indonesia
[2] Department of Electrical Engineering, Universitas Sebelas Maret, Surakarta, Indonesia
Email: mekosulistyo@staff.uns.ac.id (M.E.S.); djoksus@staff.uns.ac.id (D.D.S.); muhammad.nizam@staff.uns.ac.id (M.N.); ubaidillah_ft@staff.uns.ac.id (U.); felly.anta@student.uns.ac.id (F.A.)
*Corresponding author

***Abstract*—Bearing faults are a major cause of degradation in Brushless DC (BLDC) motors, making reliable detection of different bearing fault conditions essential for maintaining industrial equipment. This study proposes a diagnostic method that combines ReliefF feature selection with a Random Forest classifier to identify both single and compound bearing faults. Unlike earlier studies that applied this combination mainly to single-fault or binary classifications, the present work addresses a more realistic seven-class bearing fault problem. From the vibration signals, eighteen statistical features were calculated, and ReliefF was employed to identify the features that most effectively distinguish among the bearing fault categories. The resulting feature ranking improves separability, especially for compound-bearing faults that often exhibit overlapping spectral characteristics. With these selected features, the Random Forest model achieved strong diagnostic performance, demonstrating that the proposed framework offers an efficient and practical solution for identifying complex bearing fault conditions in BLDC motors.**

***Keywords*—compound fault diagnosis, Brushless DC (BLDC) motor bearings, ReliefF feature ranking, random forest classifier, vibration signal analysis, multi-class fault classification**

## I. Introduction

Electric motors now play a central role in many modern technologies, ranging from electric vehicles to automated manufacturing and precision machinery. As these applications expand, industries increasingly depend on reliable methods to detect faults before they cause operational problems [1–3]. Among the various motor types, Brushless DC (BLDC) motors continue to attract significant attention due to their efficiency, compact design, and generally low maintenance requirements. Nevertheless, these motors are not immune to mechanical or electrical issues. Failures involving bearings, stator windings, or rotor components are still frequently reported, with bearing-related problems remaining one of the primary causes of malfunction in rotating machines. Bearing deterioration can directly impact equipment safety, operational stability, and long-term reliability [4–12].

In practical industrial environments, bearing failures rarely develop as a single, isolated defect. Multiple types of damage such as spalling on the inner race, wear on the outer race, cage distortion, or rolling-element flaws can occur simultaneously. When this happens, the resulting vibration signals frequently overlap in the time–frequency domain, producing patterns that are difficult to separate or interpret [13, 14]. These compound conditions significantly complicate diagnostics and increase the risk of severe mechanical failure if left undetected. Therefore, the ability to accurately identify both single and combined bearing faults is essential to support predictive maintenance, reduce downtime, and minimize the financial impact associated with unexpected system failures [15–18].

Despite the expanding body of research on machine learning approaches for bearing fault diagnosis, several challenges remain unresolved. Many studies that combine ReliefF and Random Forest focus primarily on relatively simple scenarios, such as identifying single faults or performing binary classification. These setups do not accurately represent conditions in industrial BLDC motors, where compound faults are common and often generate overlapping or masking vibration patterns.

Another challenge concerns the use of ReliefF itself. Although this method is frequently applied for feature ranking, only a few studies have investigated its effectiveness in distinguishing informative features when vibration data originate from high-resolution BLDC measurements affected by multiple interacting faults. In contrast, Random Forest is widely recognized for its strong generalization performance; however, its integration with an optimized feature-selection process has seldom been

Manuscript received September 22, 2025; revised November 10, 2025; accepted January 9, 2026; published April 23, 2026.

explored to enhance class differentiation across various fault types.

Taken together, these limitations suggest that existing methods do not yet provide a feature-selection-driven diagnostic framework well suited for multi-class and compound fault conditions in BLDC bearings.

## II. Literature Review

### A. Fault Diagnosis

Traditional fault diagnosis techniques rely heavily on manual inspection or heuristic rule-based systems, which are often limited in scalability and adaptability [19]. Additionally, these methods use signal processing techniques to detect faults. However, they frequently encounter challenges related to feature selection, noise resilience, and generalization across varying operational conditions [20]. To address these limitations, recent studies have explored intelligent diagnostic approaches leveraging Machine Learning (ML) and Deep Learning (DL) models [21–23]. Artificial Intelligence (AI) and machine learning-based methods have emerged as powerful tools for motor fault detection by enabling automated feature extraction, fault classification, and predictive maintenance [24]. In particular, Random Forests have demonstrated great promise in fault classification tasks due to their robustness, interpretability, and strong generalization performance [20].

A critical step in developing effective fault diagnosis systems is selecting relevant features from the acquired vibration signals. High-dimensional datasets often contain redundant or irrelevant features that can degrade classification accuracy and increase computational costs [25]. Feature Selection (FS) methods aim to identify and retain only the most informative attributes, thereby enhancing model interpretability, training efficiency, and classification performance. Among various FS techniques, ReliefF has gained recognition for its ability to assess feature importance based on instance-based learning and relevance to the output class, making it particularly useful for condition monitoring tasks involving overlapping class distributions or noise [26, 27]. Recent studies have also explored heuristic and hybrid FS methods, such as metaheuristic optimization algorithms, to further refine the feature set and improve generalization across different datasets [25]. Moreover, FS plays a vital role in intelligent fault-tolerant systems by enabling more robust and adaptive diagnosis under variable or uncertain conditions [27].

### B. ReliefF Feature Selection

ReliefF is an enhanced filter-based algorithm for feature selection that measures each feature's ability to discriminate between similar samples across classes. For each randomly chosen instance $x_i$, ReliefF finds its $k$ nearest hits (same class) and $k$ nearest misses (different classes), then updates feature weights $W(j)$ as Eq. (1):

$$W(j) = W(j) - \frac{1}{m}\sum_{i=1}^{m}\left[diff(X_i^j, H^j) - diff(X_i^j, M^j)\right] \quad (1)$$

where $m$ is the number of iterations, and *diff* measures feature value differences. After scoring, the top $k$ features are selected. ReliefF's tolerance to noise and interactions makes it useful in various domains from medical imaging to remote sensing [28, 29].

### C. Random Forest Model Classifier

Random Forest is a powerful ensemble learning method used for both classification and regression tasks. It consists of multiple decision trees, each trained on a random subset of the data (bootstrapped samples) and a random subset of the features. During inference, each tree casts a vote, and the final prediction is determined by majority voting (for classification) or averaging (for regression).

Advantages of Random Forest are high accuracy and robustness to overfitting, capable of handling high-dimensional data, and built-in feature importance ranking.

The overall prediction for a sample x is given by Eq. (2):

$$\hat{y} = majority\_vote(T_1(x), T_2(x), \ldots, T_N(x)) \quad (2)$$

where $T_n(x)$ is the prediction from the n-th tree, and $N$ is the total number of trees. Random Forest also provides a measure of feature importance by evaluating how much each feature reduces impurity [30].

### D. Deep Learning or Hybrid ML Approaches Post-2024

Recent studies published after 2024 demonstrate a clear shift toward more advanced and complex learning models for vibration-based fault diagnosis. Transformer architectures (e.g., Swin Transformer), Convolutional Neural Network (CNN)-Long Short Term Memory (LSTM)-Transformer fusion models, and graph neural networks have been extensively employed in recent research [31–33]. These architectures are all capable of extracting hierarchical temporal-spectral patterns directly from vibration signals.

However, these models often face practical limitations: they require large labeled datasets, are computationally intensive, and tend to be difficult to interpret. Furthermore, few modern deep learning methods explicitly address compound-bearing faults, despite the introduction of several graph architectures [31, 34]. Challenges remain, particularly due to overlapping vibration signatures.

Due to these limitations, there is still a need for more lightweight and interpretable approaches, particularly those that integrate classical feature ranking with conventional machine learning. This approach remains relatively underexplored in the context of multi-class and compound faults in BLDC motors.

## III. Materials and Methods

### A. Experimental Setup

The vibration data analyzed in this study were experimentally collected from a 6204 bearing series mounted on a 1500-watt, 48-volt BLDC motor. The bearing conditions investigated include a healthy bearing, inner race-ball fault, outer race-ball fault, inner race-cage

fault, inner-outer race fault, and outer race-cage fault. The test apparatus is shown in Fig. 1.

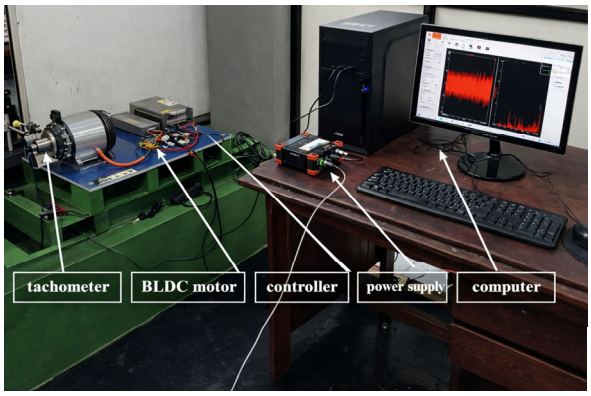


Fig. 1. Experimental setup for vibration analysis of bearing faults in BLDC motor.

Vibration measurements in this study, as shown in Fig. 1, were obtained using a PCB Piezotronics 352C33 LW23012 accelerometer. The sensor has a nominal sensitivity of 10.39 mV/mm/s² (approximately 101.8 mV/g), supports a ±50 g range, and maintains a relatively flat response from about 2 Hz to 10 kHz. It was mounted on the bearing housing at the 12 o'clock radial position, using a magnetic adapter to ensure a rigid connection and minimize additional mechanical noise. Prior to testing, the accelerometer was calibrated on a reference shaker following the ISO 16063-21 procedure.

The output signal was routed to a DeweSoft SIRIUSm-3xACC-1xACC data acquisition module and recorded using DeweSoft®. Each one-second segment of the vibration signal was then preprocessed by removing the DC offset, normalizing the amplitude, and applying a 10–5000 Hz band-pass filter to suppress low-frequency drift and high-frequency noise. No resampling or interpolation was performed. These steps were applied consistently across all bearing conditions to ensure the measurements remained comparable.

Fig. 2 illustrates seven different bearing conditions, labeled (a) through (g), each depicting a specific artificial fault. The white dotted markings in the images indicate the locations of the damage.

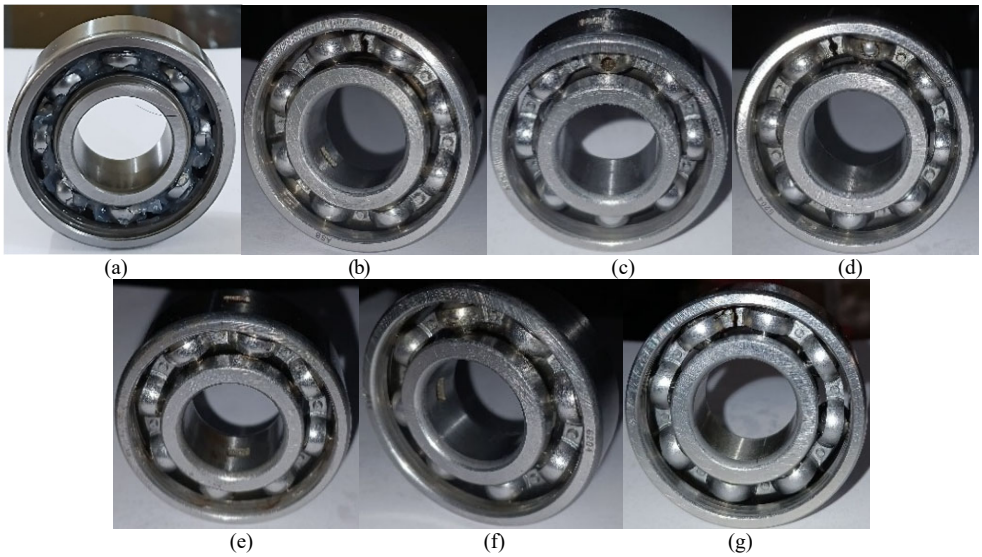


Fig. 2. Bearing artificial faults (a) normal; (b) inner race-cage fault; (c) outer race-ball fault; (d) ball-cage fault; (e) inner-outer race fault; (f) inner race-ball fault; (g) outer race-cage fault.

Artificial faults in the BLDC motor bearings were introduced using the Electrical Discharge Machining (EDM) method. Several types of defects were intentionally created, including holes or notches on the inner race and outer races measuring 2.5×5 mm, as well as ball defects in the form of 2.5 mm diameter holes. Additionally, cage faults were induced by damaging the ball-retaining structure of the bearing cage [35].

The data acquisition process in this study involved sampling vibration signals using an accelerometer sensor, which was securely mounted and connected to a Dynamic Signal Analyzer (DSA). Vibration data were collected from BLDC motors operating at a nominal speed of 2200 RPM under various bearing conditions. These conditions included normal bearings, inner race–cage faults, outer race–ball faults, ball–cage faults, combined inner–outer faults, inner race–ball faults, and outer race–cage faults.

In this study, vibration data from a BLDC motor with bearing faults were continuously recorded for one hour at a sampling rate of 10 kHz, resulting in 36 million data points. For analysis and computational efficiency, a subset of 300 one-second segments was selected. Each segment contained 10,000 samples, totaling 3,000,000 data points for subsequent processing. These segments were extracted at regular 20-second intervals to ensure a representative distribution of the motor's operating conditions throughout the recording period.

Each one-hour vibration recording was divided into one-second windows, corresponding to approximately 36.7 shaft revolutions at a motor speed of 2200 RPM. A one-second duration is commonly used in bearing analysis because it captures multiple cycles of fault-induced impacts, ensuring that each window contains a complete representation of the defect signature. To reduce statistical

dependence between adjacent windows—since vibration signals often exhibit temporal autocorrelation—the segments were sampled every 20 s rather than continuously. At this interval, more than 440 shaft revolutions occur, which helps ensure that each sampled window represents an independent realization rather than a redundant observation. A total of 300 windows per class were selected to balance dataset representativeness, statistical independence, and computational efficiency.

These samples were then divided into 70% training data and 30% testing data.

### B. Feature Extraction Method Based on Vibration Data

For each bearing condition, the one-hour vibration recording was divided into one-second segments, resulting in 3600 samples per segment. Before feature extraction, each segment was standardized using a z-score, and segments containing values exceeding approximately ±4 standard deviations were removed to prevent the influence of abnormal spikes. A Hanning window was then applied to minimize spectral leakage during frequency-domain processing.

The spectral information for each segment was computed using a 10,000-point FFT. The Power Spectral Density (PSD) was then estimated via Welch's method, applying a 50% overlap between adjacent frames. All recordings were processed using the same routine to ensure that the resulting time–frequency features remained consistent across bearing conditions and could be reliably used in the ReliefF feature-ranking stage.

## IV. Result and Discussion

### A. Raw Vibration Data

Vibration data were collected using accelerometer sensors integrated with a set of measurement instruments. The acquired signals were then processed and analyzed. Measurements were taken from two identical motors operating under various fault conditions. Fig. 3 illustrates representative raw vibration signals for each machine condition, recorded over a duration of one second.

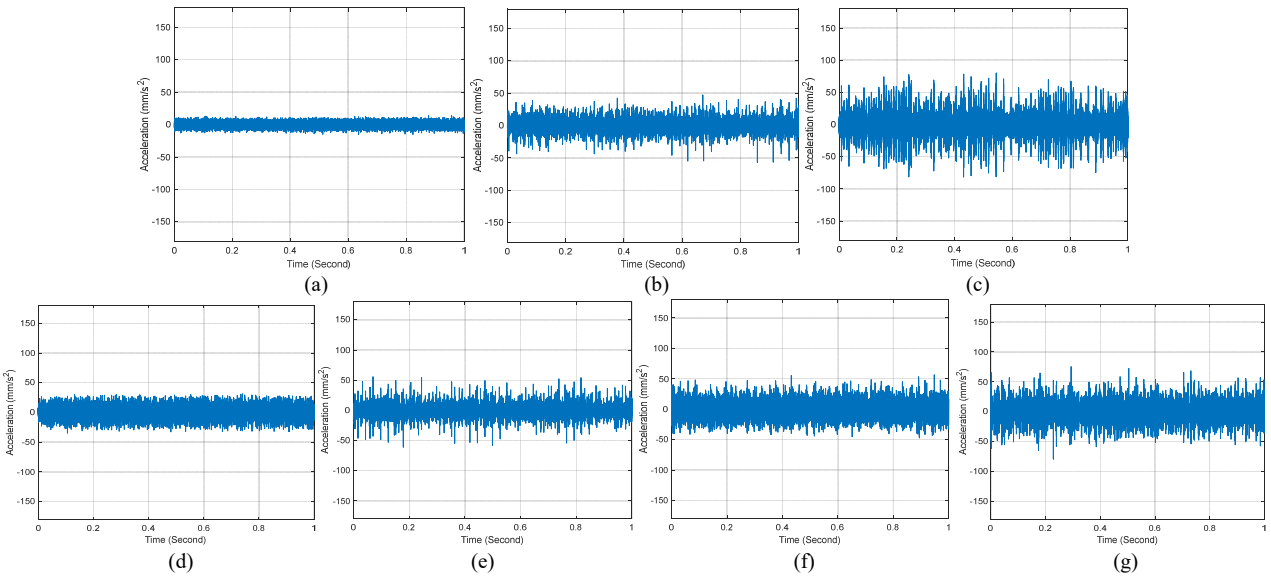


Fig. 3. Vibration signal of various bearing conditions, (a) normal; (b) inner race-cage fault; (c) outer race-ball fault; (d) ball-cage fault; (e) inner-outer race fault; (f) inner race-ball fault; (g) outer race-cage fault.

The vibration signals used in this study were collected from rolling bearings under controlled conditions. Accelerometers were attached to the bearing housing, and data were recorded at a fixed sampling rate of 10 kHz to capture detailed fault information. The dataset includes 6 bearing conditions: normal (healthy), inner race fault, outer race fault, ball fault, and two compound faults (inner–outer and inner–cage faults).

Each signal was recorded for a duration sufficient to capture multiple shaft rotations, enabling the detection of repeated fault patterns. In the time domain, normal signals appeared smooth and stable, whereas faulty bearings exhibited sudden spikes, irregular patterns, and repeated impacts. These differences result from defects within the bearing and are crucial for diagnosing bearing condition.

Although some faults could be roughly identified by examining the waveform shape, detailed analysis using feature extraction and classification was necessary to distinguish similar fault types and achieve accurate results.

### B. Feature Extraction

Three hundred vibration data samples were collected for each bearing condition, resulting in a total of 2100 datasets covering seven bearing fault conditions. The dataset was split into 70% training data and 30% testing data. The raw data obtained from vibration signal measurements were then processed into statistical parameters. The primary objective was to transform complex data into a simpler representation that still reflects the essential characteristics of the data. Eighteen statistical features were used, consisting of 12 time-domain features and 6 frequency-domain features. The results are shown in Fig. 4.

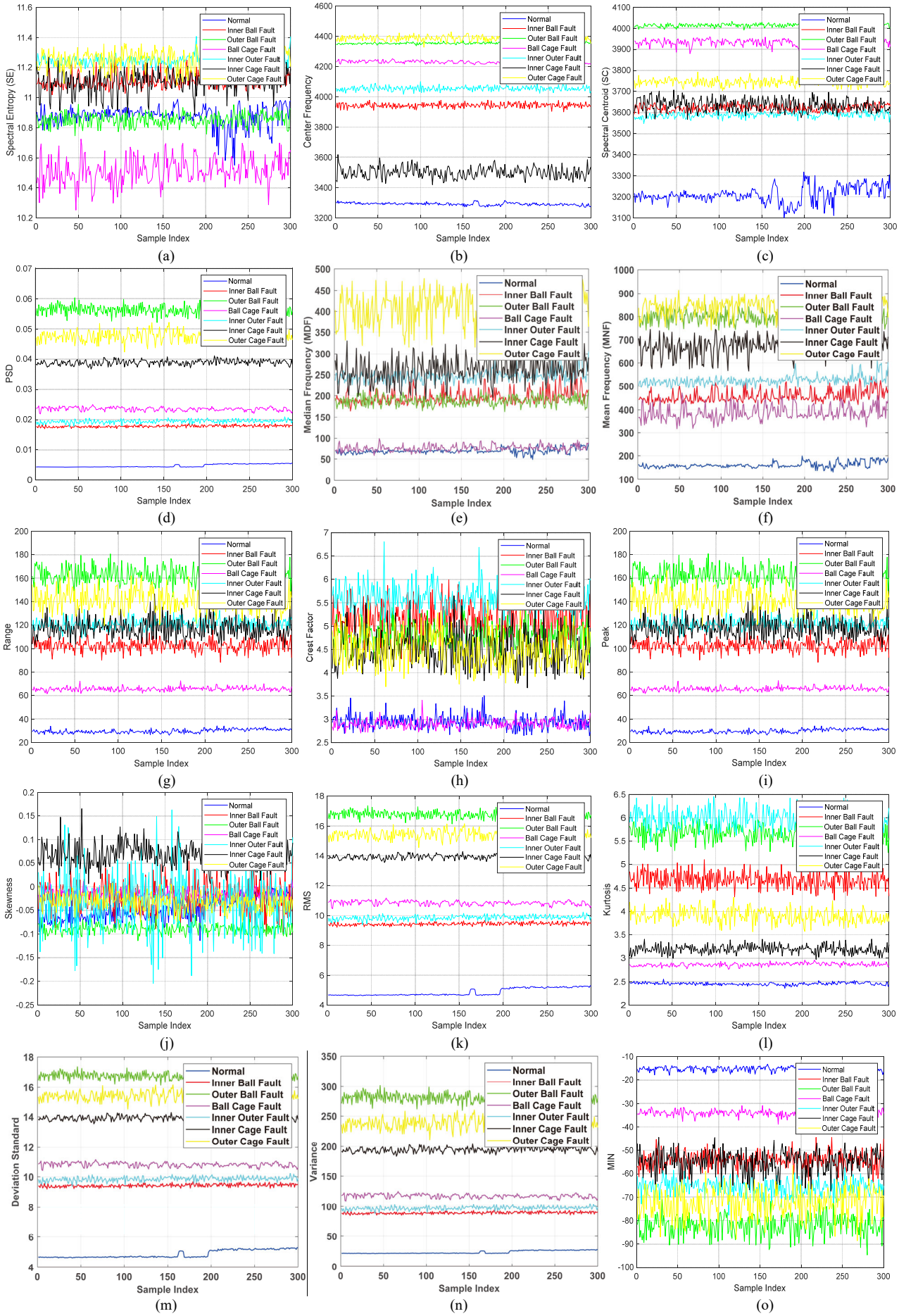
Spectral Entropy (SE)
Center Frequency
Spectral Centroid (SC)
PSD
Median Frequency (MDF)
Mean Frequency (MNF)
Range
Crest Factor
Peak
Skewness
RMS
Kurtosis
Deviation Standard
Variance
MIN
Sample Index
Normal
Inner Ball Fault
Outer Ball Fault
Ball Cage Fault
Inner Outer Fault
Inner Cage Fault
Outer Cage Fault
(a)
(b)
(c)
(d)
(e)
(f)
(g)
(h)
(i)
(j)
(k)
(l)
(m)
(n)
(o)

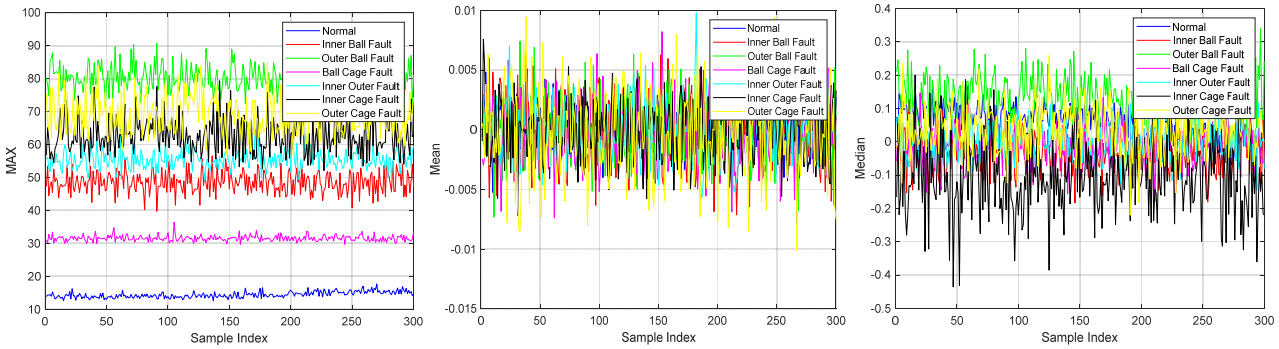


(p) (q) (r)

Fig. 4. Statistical feature extraction. (a) Spectral Entropy (SE); (b) Center Frequency; (c) Spectral Centroid (SC); (d) Power Spectral Density (PSD); (e) Median Frequency (MDF); (f) Mean Frequency (MNF); (g) range; (h) Crest Factor (CF); (i) Peak Value (PV); (j) Skewness (Skew); (k) Root Mean Square (RMS); (l) Kurtosis (Kur); (m) Standard Deviation (STD); (n) variance, (o) Minimum (Min); (p) Maximum (Max); (q) Mean; (r) Median.

To characterize the dynamic behavior of the vibration signals, a total of 18 statistical features were extracted from each segmented signal. These features were selected to capture diverse aspects of signal characteristics across both time and frequency domains. In the time domain, features such as Mean, Median, Maximum (Max), Minimum (Min), Variance, Standard Deviation (STD), Kurtosis (Kur), Root Mean Square (RMS), Skewness (Skew), Peak Value (PV), Crest Factor (CF), and Range were computed to quantify signal amplitude, symmetry, and variability. These metrics provide insight into the mechanical energy, impulsiveness, and asymmetry of vibrations caused by bearing defects. In the frequency domain, features such as Center Frequency, Mean Frequency (MNF), MDF, Spectral Entropy (SE), PSD, and Spectral Centroid (SC) were derived using Fourier transform techniques, enabling the identification of dominant frequency components and spectral energy distribution associated with fault-induced resonances.

When extracted features are used to train machine learning models such as Support Vector Machines, Random Forests, or Artificial Neural Networks, certain parameters consistently demonstrate stronger discriminative power. Features related to signal energy and dispersion—such as RMS, variance, standard deviation, range, MNF, and center frequency—tend to provide clear separation between fault classes while remaining relatively stable within the same class.

In contrast, features such as mean, median, and skewness contribute little to class separability in this dataset. Their distributions overlap substantially across different bearing conditions, indicating that they provide limited diagnostic value and may even introduce unnecessary noise into the classification process. Kurtosis and crest factor play an intermediate role; although they are less effective at distinguishing complex or compound fault types, they remain useful for detecting the early onset of impulsive behavior associated with bearing damage.

From a physical perspective in BLDC motor applications, the influence of sensor placement helps explain these observations. Faults involving the outer race, such as damage to the outer ball or outer cage, generally produce higher vibration amplitudes at the sensor location because the transmission path from the outer race to the accelerometer is relatively direct. In contrast, vibrations generated by inner-race or cage defects must propagate through rolling elements, lubrication layers, and surrounding structures, which tend to attenuate their energy before reaching the sensor.

Compound damage involving cage defects, especially when combined with inner or outer race faults, consistently exhibits greater severity in both amplitude and frequency shifts. Cage damage frequently disrupts the stability of rolling elements, causing irregular and random vibration patterns. When this instability interacts with additional race damage, the resulting vibration response becomes more intense and complex, which accounts for the elevated feature values observed under these conditions.

TABLE I. IMPORTANCE SCORE VALUE FOR EACH FEATURE

| Rank | Feature | Importance Weight |
|---|---|---|
| 1 | Center Frequency | 0.37386 |
| 2 | Variance | 0.33512 |
| 3 | PSD | 0.33512 |
| 4 | Standard Deviation | 0.33067 |
| 5 | RMS | 0.33067 |
| 6 | Kurtosis | 0.30501 |
| 7 | Spectral Centroid | 0.28910 |
| 8 | Mean Frequency (MNF) | 0.27998 |
| 9 | Peak Value | 0.24622 |
| 10 | Time Range | 0.24622 |
| 11 | Maximum Value | 0.24080 |
| 12 | Minimum Value | 0.22340 |
| 13 | Median Frequency (MDF) | 0.21403 |
| 14 | Spectral Entropy (SE) | 0.18886 |
| 15 | Crest Factor | 0.18614 |
| 16 | Skewness | 0.10661 |
| 17 | Median | 0.05579 |
| 18 | Mean | 0.02705 |

### C. *Feature Selection*

Visual inspection of Fig. 4 shows that not all features have the ability to separate the motor condition. Therefore, it needs to select the features that are sensitive to the change of the motor condition. In this paper, the ReliefF algorithm is used for feature selection. The result is shown in Table I.

The ReliefF algorithm assigns the highest weight to Center Frequency (0.37386), identifying it as the most critical feature for class separation. This suggests that fault types have distinct resonant frequency behaviors, likely due to structural variation caused by specific damage locations.

Following closely are Variance, PSD, Standard Deviation, and RMS, all time or frequency-domain features capturing energy, dispersion, and magnitude, which are crucial in identifying transient events caused by bearing defects.

On the lower end, Mean, Median, and Skewness show much smaller importance weights, indicating limited contribution to class separability. These features typically represent central tendency and asymmetry, which might not vary significantly across different fault types in this dataset.

The feature selection process clearly aids in dimensionality reduction by highlighting only the most informative attributes. Selecting the top 6–10 features from this ranked list is advisable to balance classification accuracy and computational efficiency in machine learning models.

### *D. Fault Diagnosis Using Random Forest Classifier*

Table I shows that Center Frequency, Variance, PSD, Standard Deviation, RMS, and Kurtosis give high importance scores. These features will then be selected to build the Random Forest model for multiple bearing faults diagnosis in BLDC motor. The bearing faults data are categorized as follows:

(1) Class 1: Normal Condition.
(2) Class 2: Inner-Ball Fault.
(3) Class 3: Outer-Ball Fault.
(4) Class 4: Ball-Cage Fault.
(5) Class 5: Inner–Outer Fault.
(6) Class 6: Inner–Cage Fault.
(7) Class 7: Outer Cage Fault.

The model was initially trained using the training data, and the resulting model was subsequently evaluated with the testing data. The classification results are presented in Figs. 5 and 6, displayed as a confusion matrix and a scatter plot, respectively.

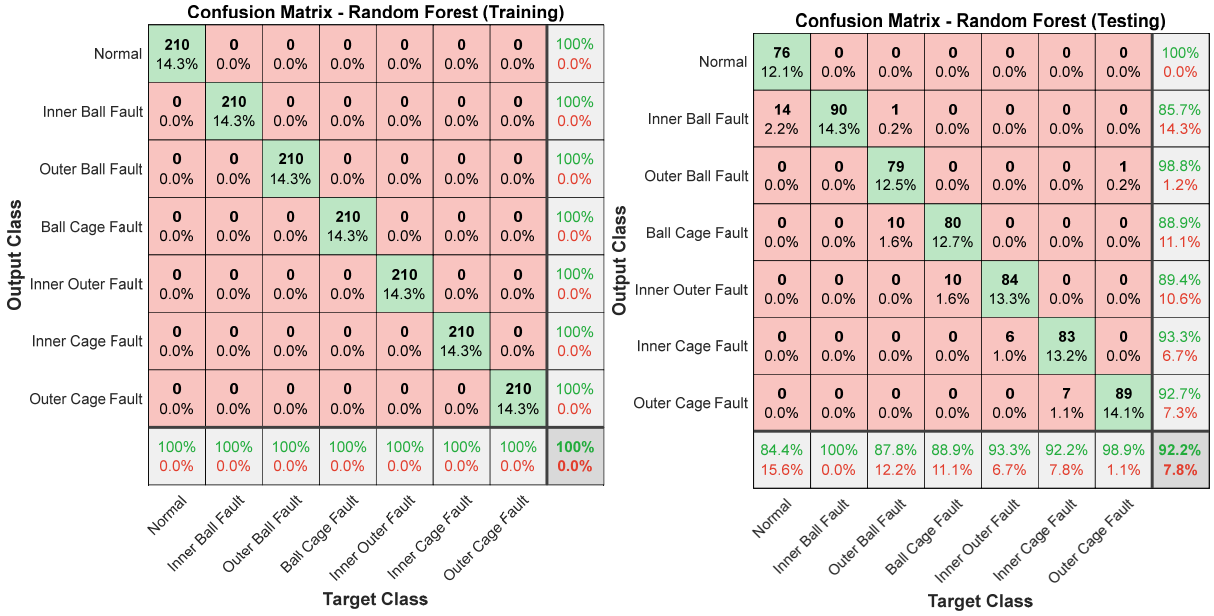


Fig. 5. Confusion matrix, (a) training data; (b) testing data.

Fig. 5 illustrate the performance of the Random Forest classifier across seven different bearing fault conditions using confusion matrices for both the training and testing datasets. During training, the model achieved perfect classification, correctly identifying all 210 samples per class, resulting in 100% training accuracy.

This indicates that the model successfully captured all relevant patterns in the training data. During the testing phase, the model maintained high performance, achieving an overall testing accuracy of 92.2%. Most classes were classified with high precision, including Normal (100%), Ball Cage Fault (88.9%), and Outer Cage Fault (92.7%).

However, some misclassifications were observed. In particular, 14 samples of Inner Ball Fault were misclassified as Normal, and a few samples from Inner–Outer Fault and Inner Cage Fault were misclassified among each other. These confusions likely stem from overlapping features in the compound fault signatures.

Despite this, the classifier demonstrated strong generalization and fast computation time (1.29 s), confirming its effectiveness for multi-class bearing fault classification using vibration data.

The classification results for bearing fault conditions with various types are illustrated using scatter plots, as shown in Fig. 6. These scatter plots utilize Center Frequency and Kurtosis features to visualize data distribution and emphasize the separability among different fault classes.

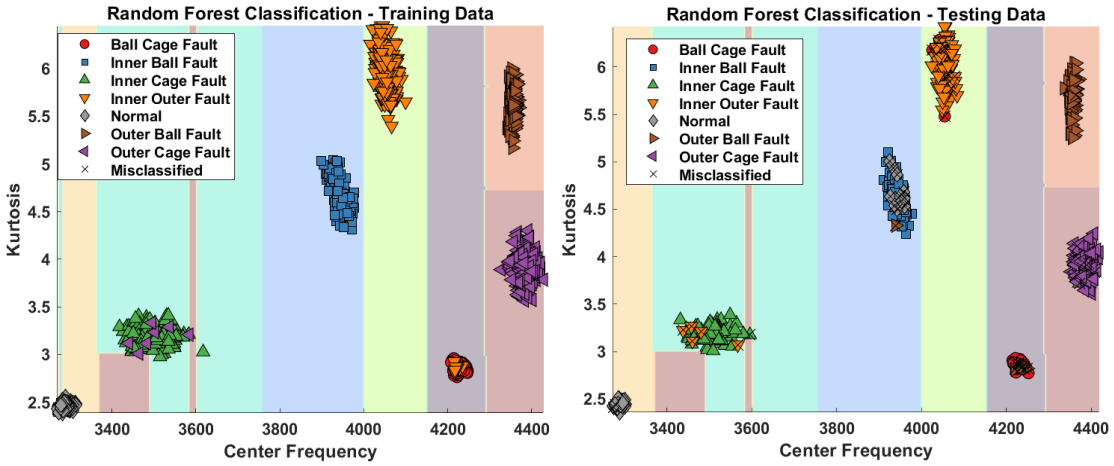


(a) (b)

Fig. 6. Scatter plot using random forest classifier based on center frequency & Kurtosis features, (a) training data; (b) testing data.

Fig. 6 shows the scatter plot of the Random Forest classification results on the training data for seven bearing fault classes. The plot uses Center Frequency and Kurtosis features to visualize the separation between classes. Each fault type is represented with distinct markers and colors, enabling clear visual distinction. The distribution of data points indicates that the Random Forest model successfully clustered the samples by class, with no visible misclassifications in the training set. This result confirms the model's ability to effectively learn fault-specific patterns during training.

The strong performance of the ReliefF-Random Forest approach in this study arises not solely from the algorithm itself but from the complementary strengths of both methods. For example, ReliefF consistently identified features that engineers typically associate with bearing deterioration, such as kurtosis, crest factor, and spectral entropy. These features tend to amplify the subtle yet meaningful impulsive signatures that emerge when a defect begins to develop on the inner race or rolling element.

Once these features were selected, the Random Forest algorithm handled the classification task with a high degree of stability. Because this method relies on an ensemble of decision trees rather than a single model, it is inherently more tolerant of noise, small amplitude fluctuations, and the irregularities commonly found in real vibration data. In practice, this makes the model easier to work with compared to Support Vector Machines (SVM) or Artificial Neural Networks (ANN), which typically require careful tuning to perform optimally.

The remaining misclassifications primarily occurred in compound faults, such as combinations of ball–inner race and cage–outer race defects. These results are unsurprising, as several previous studies have reported that interacting defects tend to generate overlapping vibration patterns that are difficult to separate clearly. This limitation also highlights an opportunity for future research, potentially through the incorporation of deep learning models capable of automatically identifying more subtle frequency–time patterns.

Overall, the findings indicate that the ReliefF-Random Forest combination offers a practical middle ground: it is computationally efficient, interpretable, and sufficiently accurate for use in a real monitoring setup for BLDC motor bearings.

### *E. Comparison of Random Forest, SVM, ANN, and CNN*

Various algorithms have been employed to detect bearing failures, including SVM, ANN, and several CNN-based models [36–38]. However, for the dataset used in this study, the Random Forest algorithm proved to be more suitable. This method is notably stable even with small datasets, is not overly sensitive to parameter settings, and effectively handles nonlinear feature relationships. Additionally, Random Forest provides insights into the importance of each feature, which is valuable for interpreting model behavior [39].

Although the ReliefF-Random Forest approach performed well in this study, several considerations should be noted before applying the method more broadly. The experiments were conducted in a controlled laboratory setting, with the motor operating at a single, steady speed. In real industrial environments, however, motors rarely function under such fixed conditions; variations in load, temperature, or mechanical disturbances can affect vibration features and introduce variability that may reduce the classifier's accuracy. Additionally, the current analysis relies heavily on manually engineered statistical features. While these features are intuitive and straightforward to compute, they may be insufficient for capturing subtle nonlinear patterns that deep learning methods are often better suited to identify.

An additional challenge arises when dealing with compound faults. Since the vibration signals generated by multiple defects often overlap, the boundaries between classes are not always distinct, which explains why some cases were misclassified. Furthermore, the dataset is derived from a limited number of motors, making it uncertain how well the model would generalize to different motor types or larger industrial environments. For future work, it would be valuable to test the method across varying speeds and loads, incorporate data from more motor units, and explore hybrid or deep learning

techniques to enhance robustness and improve the quality of feature extraction.

## V. Conclusion

The bearing fault diagnosis framework for BLDC motors proposed in this study combines a Random Forest classifier with ReliefF feature ranking. ReliefF was used to rank statistical features extracted from vibration signals. It identified parameters related to energy and frequency-such as center frequency, power spectral density, variance, and RMS-as the most discriminative, while basic statistical features contributed minimally. Despite slight misclassification among compound fault classes because of overlapping vibration characteristics, the Random Forest classifier, using the selected features, achieved high accuracy across seven bearing conditions, including single and compound faults. The model attained a testing accuracy of 92.2%—despite measurement noise and variability, demonstrating robust performance in less-than-ideal conditions. The ReliefF-Random Forest technique offers a favorable balance of accuracy, interpretability, and computing efficiency when compared to SVM, ANN, and CNN methodologies. Future research will validate the proposed framework's performance under various operating speeds, loads, and environmental conditions to improve its generalization and practical deployment. Additionally, multi-sensor data-such as temperature, current, or acoustic signals-will be incorporated to enhance fault sensitivity.

## Conflict of Interest

The authors declare no conflict of interest.

## Author Contributions

MES conducted the experimental work, performed data analysis, and prepared the manuscript; DDS provided resources, supervised the research, and revised the final manuscript; MN assisted with data processing and validation; U evaluated the research results and reviewed the manuscript; FA prepared the test rig and data acquisition system; all authors had approved the final version.

## Funding

This research was funded by Sebelas Maret University through the Doctoral Postgraduate Research funding scheme, grant number: 371/UN27.22/PT.01.03/2025.

## Acknowledgment

The authors would like to express their sincere gratitude to Sebelas Maret University for providing financial support for this research. The support and facilities provided by the university have been invaluable in enabling the successful completion of this study. The authors also like to acknowledge Endriyanto, and Dhafa Dhiya for their support and contributions throughout the experimental work.

## References

[1] W. Qiu, X. Zhao, A. Tyrrell *et al.,* "Application of artificial intelligence-based technique in electric motors: A review," *IEEE Transactions on Power Electronics*, vol. 39, no. 10, pp. 13543–13568, 2024. doi: 10.1109/TPEL.2024.3410958

[2] Y. Hu, X. Zhang, and W. Lang, *AI Techniques in EV Motor and Inverter Fault Detection and Diagnosis*, The Institution of Engineering and Technology, 2023.

[3] D. D. Susilo, Ubaidillah, A. R. Prabowo *et al.,* "Diagnosing of BLDC motor faults based on LSSVM model and vibration signal," *E3S Web of Conferences*, vol. 465, 01024, 2023. doi: 10.1051/e3sconf/202346501024

[4] A. Almounajjed, A. K. Sahoo, M. K. Kumar *et al.,* "Stator fault diagnosis of induction motor based on discrete wavelet analysis and neural network technique," *Chinese Journal of Electrical Engineering*, vol. 9, no. 1, pp. 142–157, 2023. doi: 10.23919/CJEE.2023.000003

[5] J. Rengifo, J. Moreira, F. Vaca-Urbano *et al.,* "Detection of inter-turn short circuits in induction motors using the current space vector and machine learning classifiers," *Energies*, vol. 17, no. 10, 2241, 2024. doi: 10.3390/en17102241

[6] P. Gangsar and R. Tiwari, "Signal based condition monitoring techniques for fault detection and diagnosis of induction motors: A state-of-the-art review," *Mechanical Systems and Signal Processing*, vol. 144, 106908, 2020. doi: 10.1016/j.ymssp.2020.106908

[7] C. He, P. Han, J. Lu *et al.,* "Real-time fault diagnosis of motor bearing via improved cyclostationary analysis implemented onto edge computing system," *IEEE Transactions on Instrumentation and Measurement*, vol. 72, 3524011, 2023. doi: 10.1109/TIM.2023.3295476

[8] C. Li, L. Ledo, M. Delgado *et al.,* "A Bayesian approach to consequent parameter estimation in probabilistic fuzzy systems and its application to bearing fault classification," *Knowledge-Based Systems*, vol. 129, pp. 39–60, 2017. doi: 10.1016/j.knosys.2017.05.007

[9] C. Li, J. V. de Oliveira, M. Cerrada *et al.,* "Observer-biased bearing condition monitoring: From fault detection to multi-fault classification," *Engineering Applications of Artificial Intelligence*, vol. 50, pp. 287–301, 2016. doi: 10.1016/j.engappai.2016.01.038

[10] Y. Du, X. Geng, Q. Zhou *et al.,* "A fault diagnosis method for offshore wind turbine bearing based on adaptive deep echo state network and bidirectional long short term memory network in noisy environment," *Ocean Engineering*, vol. 312, 119101, 2024. doi: 10.1016/j.oceaneng.2024.119101

[11] C. Li, J. Zheng, H. Pan *et al.,* "Refined composite multivariate multiscale dispersion entropy and its application to fault diagnosis of rolling bearing," *IEEE Access*, vol. 7, pp. 47663–47673, 2019. doi: 10.1109/ACCESS.2019.2907997

[12] J. Niu, S. Lu, Y. Liu *et al.,* "Intelligent bearing fault diagnosis based on tacholess order tracking for a variable-speed AC electric machine," *IEEE Sensors Journal*, vol. 19, no. 5, pp. 1850–1861, 2019. doi: 10.1109/JSEN.2018.2883955

[13] L. Chen, A. Tan, L. Yang *et al.,* "Defect size evaluation of cylindrical roller bearings with compound faults on the inner and outer races," *Mathematical Problems in Engineering*, vol. 2022, no. 1, 6070822, 2022. doi: 10.1155/2022/6070822

[14] N. D. Thuan and H. S. Hong, "HUST bearing: A practical dataset for ball bearing fault diagnosis," *BMC Research Notes*, vol. 16, no. 1, 138, 2023. doi: 10.1186/s13104-023-06400-4

[15] T. A. Shifat and J.-W. Hur, "ANN assisted multi sensor information fusion for BLDC motor fault diagnosis," *IEEE Access*, vol. 9, pp. 9429–9441, 9317859, 2021. doi: 10.1109/ACCESS.2021.3050243

[16] C. Chen, Y. Yuan, and F. Zhao, "Intelligent compound fault diagnosis of roller bearings based on deep graph convolutional network," *Sensors*, vol. 23, no. 20, 8489, 2023. doi: 10.3390/s23208489

[17] J. Blesa, J. Quevedo, V. Puig *et al.,* "Fault diagnosis and prognosis of a brushless DC motor using a model-based approach," in *Proc. the European Conf. of the Prognostics and Health Management Society*, 2020, vol. 5, no. 1. doi: 10.36001/phme.2020.v5i1.1257

[18] R. Zhao, R. Yan, Z. Chen *et al.,* "Deep learning and its applications to machine health monitoring," *Mechanical Systems and Signal Processing*, vol. 115, pp. 213–237, 2019. doi: 10.1016/j.ymssp.2018.05.050

[19] Y. Chen, J. Chen, Y. Qiang *et al.,* "Refined composite moving average fluctuation dispersion entropy and its application on rolling bearing fault diagnosis," *Review of Scientific Instruments*, vol. 94, no. 10, 105110, 2023. doi: 10.1063/5.0165430

[20] Y. Liu, J. Geng, Y. Li *et al.,* "Identification of mechanical fault of induction motor by combining lyapunov exponent and random forest algorithm," in *Proc. ASME 2022 International Mechanical Engineering Congress and Exposition*, 2023, vol. 5, V005T07A094. doi: 10.1115/IMECE2022-94758

[21] S. Zhang, S. Zhang, B. Wang *et al.,* "Deep learning algorithms for bearing fault diagnostics—a comprehensive review," *IEEE Access*, vol. 8, pp. 29857–29881, 2020. doi: 10.1109/ACCESS.2020.2972859

[22] D. Neupane and J. Seok, "Bearing fault detection and diagnosis using case western reserve university dataset with deep learning approaches: A review," *IEEE Access*, vol. 8, pp. 93155–93178, 2020. doi: 10.1109/ACCESS.2020.2990528

[23] K. You, G. Qiu, and Y. Gu, "Rolling bearing fault diagnosis using hybrid neural network with principal component analysis," *Sensors*, vol. 22, no. 22, 8906, 2022. doi: 10.3390/s22228906

[24] R. Jigyasu, V. Shrivastava, and S. Singh, "Deep optimal feature extraction and selection-based motor fault diagnosis using vibration," *Electrical Engineering*, vol. 106, no. 5, pp. 6339–6358, 2024. doi: 10.1007/s00202-024-02356-1

[25] M. R. Al-Eiadeh, R. Qaddoura, and M. Abdallah, "Investigating the performance of a novel modified binary black hole optimization algorithm for enhancing feature selection," *Applied Science*s, vol. 14, no. 12, 5207, 2024. doi: 10.3390/app14125207

[26] D. Domingo, A. B. Kareem, C. N. Okwuosa *et al.,* "Transformer core fault diagnosis via current signal analysis with pearson correlation feature selection," *Electronics*, vol. 13, no. 5, 926, 2024. doi: 10.3390/electronics13050926

[27] A. A. Amin, M. S. Iqbal, and M. H. Shahbaz, "Development of intelligent fault-tolerant control systems with machine learning, deep learning, and transfer learning algorithms: A review," *Expert Systems with Applications*, vol. 238, 121956, 2024. doi: 10.1016/j.eswa.2023.121956

[28] R. Vishraj, S. Gupta, and S. Singh, "Evaluation of feature selection methods utilizing random forest and logistic regression for lung tissue categorization using HRCT images," *Expert Systems*, vol. 40, no. 8, e13320, 2023. doi: 10.1111/exsy.13320

[29] S. Saha and D. Nandi, "SVM-RLF-DNN: A DNN with reliefF and SVM for automatic identification of COVID from chest X-ray and CT images," *Digital Health*, vol. 10, pp. 1–16, 2024. doi: 10.1177/20552076241257045

[30] A. S. Saud, S. Shakya, and B. Neupane, "Analysis of depth of entropy and GINI index based decision trees for predicting diabetes," *Indian Journal of Computer Science*, vol. 6, no. 6, pp. 19–28, 2021. doi: 10.17010/ijcs/2021/v6/i6/167641

[31] J. Ma, J. Huang, S. Liu *et al.,* "A self-attention legendre graph convolution network for rotating machinery fault diagnosis," *Sensors*, vol. 24, no. 17, 5475, 2024. doi: 10.3390/s24175475

[32] X. Yuan and W. Wu, "A bearing fault diagnosis method based on fusion of CNN-BiLSTM-transformer and cross-attention," *Academic Journal of Science and Technology*, vol. 14, no. 2, pp. 191–199, 2025. doi: 10.54097/594q8441

[33] F. Li, Y. Li, and D. Wang, "Rolling bearing fault diagnosis via temporal-graph convolutional fusion," *Sensors*, vol. 25, no. 13, 3894, 2025. doi: 10.3390/s25133894

[34] Q. Zhou, L. Xue, J. He *et al.,* "A rotating machinery fault diagnosis method based on dynamic graph convolution network and hard threshold denoising," *Sensors*, vol. 24, no. 15, 4887, 2024. doi: 10.3390/s24154887

[35] C. Lessmeier, J. K. Kimotho, D. Zimmer *et al.,* "Condition monitoring of bearing damage in electromechanical drive systems by using motor current signals of electric motors: A benchmark data set for data-driven classification," in *Proc. the European Conf. of the Prognostics and Health Management Society*, 2016, vol. 3, no. 1.

[36] N. T. H. Thu, P. N. Van, and H. Q. Hung, "Bearing fault diagnosis by machine learning and deep learning-based models: A comparative study applying for HUST bearing dataset," *Journal of Military Science and Technology*, vol. 103, 2025. doi: 10.54939/1859-1043.j.mst.103.2025.31-39

[37] W. Xie, Z. Li, Y. Xu *et al.,* "Evaluation of different bearing fault classifiers in utilizing CNN feature extraction ability," *Sensors*, vol. 22, no. 9, 3314, 2022. doi: 10.3390/s22093314

[38] R. Liang, W. Ran, Y. Chen *et al.,* "Fault diagnosis method for rotating machinery based on multi-scale features," *Chinese Journal of Mechanical Engineering*, vol. 36, no. 1, 141, 2023. doi: 10.1186/s10033-023-00966-7

[39] Q. Zhang, Y. Yao, Y. Huang *et al.,* "A bearing fault diagnosis model based on a simplified wide convolutional neural network and Random Forrest," *Sensors*, vol. 25, no. 3, 752, 2025. doi: 10.3390/s25030752